Endocytic delivery of lipocalin-siderophore-iron complex rescues the kidney from ischemia-reperfusion injury

Kiyoshi Mori,[1] H. Thomas Lee,[2] Dana Rapoport,[1] Ian R. Drexler,[1] Kirk Foster,[3] Jun Yang,[1] Kai M. Schmidt-Ott,[1] Xia Chen,[1] Jau Yi Li,[1] Stacey Weiss,[1] Jaya Mishra,[4] Faisal H. Cheema,[5] Glenn Markowitz,[3] Takayoshi Suganami,[6] Kazutomo Sawai,[6] Masashi Mukoyama,[6] Cheryl Kunis,[1] Vivette D'Agati,[3] Prasad Devarajan,[4] and Jonathan Barasch[1]

[1]Department of Medicine, [2]Department of Anesthesiology, and [3]Department of Pathology, College of Physicians and Surgeons, Columbia University, New York, New York, USA. [4]Department of Pediatrics, Nephrology and Hypertension, Cincinnati Children's Hospital, Cincinnati, Ohio, USA. [5]Department of Surgery, College of Physicians and Surgeons, Columbia University, New York, New York, USA. [6]Department of Medicine and Clinical Science, Kyoto University Graduate School of Medicine, Kyoto, Japan.

Neutrophil gelatinase–associated lipocalin (Ngal), also known as siderocalin, forms a complex with iron-binding siderophores (Ngal:siderophore:Fe). This complex converts renal progenitors into epithelial tubules. In this study, we tested the hypothesis that Ngal:siderophore:Fe protects adult kidney epithelial cells or accelerates their recovery from damage. Using a mouse model of severe renal failure, ischemia-reperfusion injury, we show that a single dose of Ngal (10 μg), introduced during the initial phase of the disease, dramatically protects the kidney and mitigates azotemia. Ngal activity depends on delivery of the protein and its siderophore to the proximal tubule. Iron must also be delivered, since blockade of the siderophore with gallium inhibits the rescue from ischemia. The Ngal:siderophore:Fe complex upregulates heme oxygenase-1, a protective enzyme, preserves proximal tubule N-cadherin, and inhibits cell death. Because mouse urine contains an Ngal-dependent siderophore-like activity, endogenous Ngal might also play a protective role. Indeed, Ngal is highly accumulated in the human kidney cortical tubules and in the blood and urine after nephrotoxic and ischemic injury. We reveal what we believe to be a novel pathway of iron traffic that is activated in human and mouse renal diseases, and it provides a unique method for their treatment.

Introduction

Acute tubular necrosis (ATN) is a syndrome characterized by loss of function and death of the proximal tubule of the kidney (1–3). The syndrome is induced by the accumulation of low–molecular weight molecules such as pharmaceuticals, by proteins filtered from the glomerulus, or by hypoxia followed by reperfusion.

A mechanism that may underlie each of these inciting factors is mislocalized iron. Unbound iron can catalyze the conversion of H_2O_2 to OH and OH^- (the Haber-Weiss reaction) or form reactive ferryl or perferryl species (4). These ions mutagenize many types of molecules, including lipids, nucleotides, and the DNA backbone (5, 6). Catalytic iron in urine or blood and peroxidized lipids have been documented in acute renal failure mediated by hemoglobin and myoglobin (7), chemotherapy (cisplatin, ref. 8; doxorubicin, ref. 9), ischemia-reperfusion (10, 11), transplant ischemia (12), and proteinuria induced tubular damage (13). Preloading animals with iron (14) worsens the disease, and, conversely, chelating iron with deferoxamine (DFO) (8, 15–19) or bacterial siderophores (20) blunts the damage. Iron-catalyzed damage is thought to be one of the earliest events in kidney dysfunction and is likely to be important in other organs, including the heart (20) and the liver (21).

Cells acquire iron from carrier proteins (transferrin) or from cell surface iron transporters (divalent metal transporter) (1, 22). Intracellular iron is controlled by the actions of the iron-responsive proteins (IRPs 1 and 2) (23–26), the ferritin complex (27–30), and heme oxygenase-1 (HO-1) (31). Because IRPs are modulated by hypoxia (32), oxidative stress (33, 34), and phosphorylation (35), changes in their activity may play an important role in ischemic disease, particularly by regulating the expression of ferritin (36–38). However, few other aspects of iron trafficking, storage, or metabolism are known in ischemic cells or in other types of tissue damage, despite the primacy of catalytic iron in their pathogenesis.

We recently identified a protein that induced the conversion of rat kidney progenitors into epithelia, tubules, and complete nephrons. The protein is called neutrophil gelatinase–associated lipocalin (Ngal) or lipocalin 2 (39), a member of the lipocalin superfamily. These proteins are composed of 8 β-strands that form a β-barrel enclosing a calyx (40). The calyx binds and transports low–molecular weight chemicals. The best evidence for Ngal's ligand comes from crystallographic studies that demonstrated a bacterial siderophore (enterochelin) in the calyx (41). Ngal binds the siderophore with high affinity (0.4 nM), and the siderophore traps iron with high affinity (10^{-49} M) (42). The stoichiometry of protein:siderophore:Fe is 1:1:1, as demonstrated by binding studies and x-ray crystallography (41). When the siderophore was loaded with iron, the Ngal complex could donate iron to cell lines and to embryonic mesenchyme in vitro, and when the siderophore was iron free, the Ngal complex could chelate iron (39, 43). In many types of cells, Ngal trafficked to a late endosomal compartment
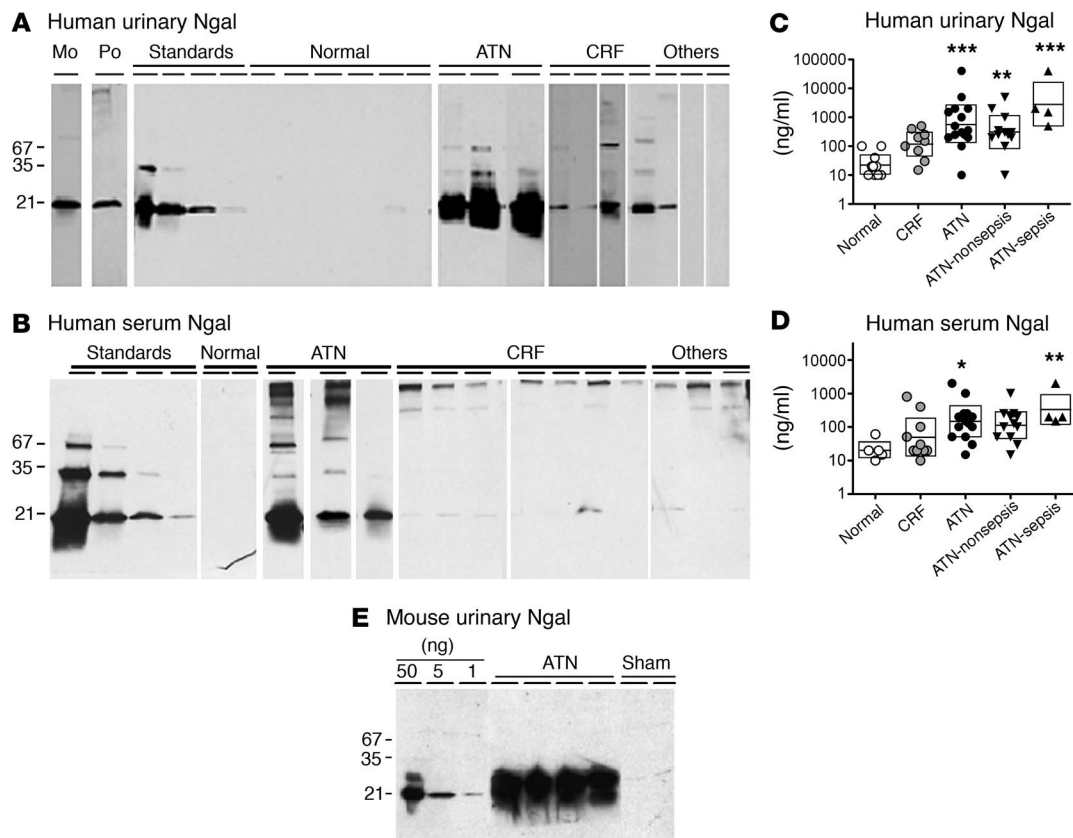
Figure 1
Ngal expression in ATN of human (**A**–**D**) and mouse (**E**). (**A**) Monoclonal anti–human Ngal (Mo) and polyclonal anti–mouse Ngal (Po) antibodies recognized recombinant (21-kDa) and native (25-kDa) human and mouse Ngal. Occasionally, higher–molecular weight species (approximately 35 kDa and 66 kDa) were present in recombinant and native preparations; these might represent dimers and trimers of Ngal. A standard curve was constructed with 25, 5, 1, and 0.2 ng recombinant proteins on nonreducing gels. Human urine samples (0.1–20 μl) from patients with ATN showed high levels of Ngal, whereas samples from patients with chronic renal failure (CRF), patients with liver cirrhosis, hemochromatosis, or pancreatic carcinoma but lacking a renal diagnosis (Others), or normal subjects (Normal) had low levels of Ngal. (**B**) Similar data were obtained from human serum. (**C** and **D**) Geometric means (bar ± SD) of urinary (**C**) and serum (**D**) Ngal were compared in normal, CRF, and ATN groups. ATN was further divided into sepsis and nonsepsis. *$P < 0.05$, **$P < 0.01$, ***$P < 0.001$ vs. normal. (**E**) Mouse ATN was also associated with elevated urinary Ngal. The renal pedicle was cross-clamped for 30 minutes, and urine was collected at 24 hours of reperfusion and analyzed by immunoblot (5 μl/lane).

that differed from the transferrin compartment (39). Because Ngal is the first mammalian protein found to bind and transport a bacterial siderophore, it has been renamed siderocalin (41).

The current work was prompted by our recent finding that Ngal is one of the most highly expressed messages and proteins in the mouse kidney after ischemia-reperfusion injury (ATN) (44, 45). Here we find that Ngal protein accumulates in the proximal tubule of human kidneys after ischemic and toxic ATN, just as in the mouse. To determine whether Ngal is protective, we injected mice with microgram quantities of the protein and found dramatic preservation of kidney histology, as well as normalized serum creatinine. The mechanism of protection required the delivery of siderophore:Fe to the proximal tubule.

Results

Expression of Ngal in ATN of the human. Acute renal failure in humans was marked by log-order elevations in the concentration of serum and urinary Ngal protein. Compared with the Ngal concentration in normal serum (21 ng/ml geometric mean; $n = 5$) and normal urine

(22 ng/ml; $n = 10$), serum Ngal was elevated 7.3-fold (146 ng/ml; $P < 0.05$; Figure 1) and urinary Ngal was elevated 25-fold (557 ng/ml; $P < 0.001$) in our patients with ATN, the most typical form of acute renal failure. Patients with ATN associated with bacterial infection tended to have the highest levels of serum Ngal (331 ng/ml) and urinary Ngal (2,786 ng/ml), but this was not statistically different from ATN without infection. To determine whether Ngal expression correlated with the extent of acute renal impairment, we used simple regression analysis after log transformation of Ngal levels. We found that both serum Ngal ($r = 0.64$, $n = 32$) and urinary Ngal ($r = 0.68$, $n = 38$), as well as urinary Ngal normalized for urinary creatinine ($r = 0.67$, $n = 36$), were highly correlated with serum creatinine levels ($P < 0.0001$ each). In comparison, patients with chronic renal failure had less prominent elevations in serum Ngal (49 ng/ml; $n = 10$) and urinary Ngal (119 ng/ml; $n = 9$), and these values were not proportional to serum creatinine. These data correlate Ngal expression with acute kidney damage, implicating the kidney as the major source of serum and urinary Ngal. Indeed, in several cases of severe renal failure, the fractional excretion of Ngal (the clearance of Ngal,

normalized for the clearance of creatinine) was greater than 100%, demonstrating that urinary Ngal derived from local synthesis, rather than only from filtration from the blood.

To visualize Ngal protein, we immunostained human samples with affinity-purified anti-Ngal polyclonal antibody (Figure 2). The normal kidney demonstrated weak staining in the distal tubular epithelia (mean 10% of cortical area) and in the medullary collecting ducts, implicating these tubules as the site of synthesis in the normal kidney. Only rare staining of glomerular parietal epithelial cells, but not other glomerular cells, was also identified. Proximal tubules were entirely negative in normal kidneys. In contrast, nearly 50% of cortical tubules, including proximal tubules, were Ngal+ in ischemic or nephrotoxin-damaged kidneys (Figure 2). Proliferative glomerulopathies also generated Ngal+ cortical tubules, but the intensity of staining and the percentage of the cortical parenchyma that were affected were much less than in ischemic disease (Ngal+ cortical parenchyma: 20% in minimal-change disease, 40% in diabetic nephropathy, 50% in anti-neutrophil cytoplasmic antibody–associated glomerulonephritis, and 65% in anti–glomerular basement membrane disease); in these cases Ngal perhaps reflects a mild degree of tubular damage by proteinuria or hemodynamic change. Those tubular cells displaying the most obvious features of cell injury, including simplification and enlarged reparative nuclei with prominent nucleoli, had the most intense staining. Tubular cells with less derangement had much less staining. These data demonstrate de novo and widespread Ngal reactivity in cortical tubules of different renal diseases, suggesting that Ngal is a common and sensitive response to tubular injury.

Exogenous Ngal rescues the mouse proximal tubule from ATN. To examine the functional significance of Ngal expression in renal ischemia, we first reproduced a common model of renal damage (44, 46) but used mice. The renal pedicle was clamped for 30 minutes, and the contralateral kidney was removed. Twenty-four hours after reperfusion, the plasma creatinine rose from 0.41 ± 0.10 mg/dl ($n = 4$) to 3.16 ± 0.17 mg/dl ($n = 8$, $P < 0.001$), and Ngal message and protein were intensely expressed. Ngal message rose approximately 1,000-fold, reducing the threshold for detection by real-time RT-PCR from 17.7 ± 0.9 cycles in sham-operated kidneys to 7.5 ± 0.4 cycles in ischemic kidneys (normalized to β-actin, ΔCT; $n = 4$ each, $P < 0.0001$). Ngal protein rose 1,000-fold in the urine (40 μg/ml in ATN compared with 40 ng/ml in the sham-operated and normal mouse; Figure 1E) and 300-fold in the blood (30 μg/ml in ATN compared with 100 ng/ml in the sham-operated mouse) and was

elevated close to 100-fold in kidney extracts (73 ± 7 μg/g compared with <1 μg/g kidney wet weight in sham-operated kidneys; $n = 3$ each, $P < 0.05$). Renal Ngal protein correlated well with the duration of cross-clamping.

Prior work showed that Ngal appeared in the urine a number of hours after ischemia-reperfusion injury (44). To determine whether Ngal protein was protective, we introduced Ngal systemically (1–300 μg by s.c. or i.p. injection) in the early stages of ATN. Introduction of 100 μg Ngal 15 minutes before clamping blocked the rise in plasma creatinine measured 24 hours after reperfusion (1.18 ± 0.18 mg/dl in Ngal-treated mice, $n = 7$, compared with 3.16 ± 0.17 mg/dl in untreated animals, $n = 8$; $P < 0.001$). Similar data were obtained for dosages ranging from 10 to 300 μg of Ngal, but 1 μg Ngal was not protective (creatinine 3.09 ± 0.11 mg/dl; $n = 3$). Introduction of Ngal 1 hour after reperfusion also blocked the azotemia (creatinine 1.60 ± 0.28 mg/dl; $n = 3$, $P < 0.001$), but to a lesser degree than pretreatment with Ngal. In contrast to these studies, treatment with Ngal 2 hours after ischemia had no protective effect (creatinine 3.12 ± 0.35 mg/dl; $n = 3$). The data were confirmed by measurement of the blood urea nitrogen (data not shown).

The protective activity of Ngal was equally measurable by histology (Figure 3): rather than necrotic tubules and luminal debris, normal epithelial morphology was preserved in the S1 and S2 segments of the proximal tubule. The S3 segment in the outer stripe of the outer medulla, however, was less protected by injection of Ngal, but tubular casts were also less evident at this site (Figure 3B). These observations were supported by scoring of the sections on the Jablonski scale (47) (Figure 3C).

Correlates of ischemia-reperfusion injury. Because the trafficking and metabolism of the cadherins are rapidly affected by ischemia (48), and because Ngal acts as an inducer of E-cadherin in rat embryonic metanephric mesenchyme (39), we hypothesized that Ngal rescues

Figure 2
Ngal is expressed in cortical tubules in human acute renal failure. Ngal was detected with affinity-purified polyclonal antibody. (**A**) The normal kidney had little staining for Ngal. (**B** and **C**) At high power, focal staining of distal tubule cells (occupying 10% of the cortical area) and collecting ducts was found. There was no staining of proximal tubules. (**D**–**I**) Ischemic ATN caused by sepsis (**D**), by hypovolemia due to vomiting and diarrhea (**E**), or by heart failure (**F**), or nephrotoxic ATN caused by bisphosphonate (**G**), by cephalosporin (**H**), or by hemoglobinuria (**I**), produced intense staining of nearly 50% of the cortical tubules. Staining was heterogeneous and most intense in epithelial cells that displayed histologic features of cell injury, including simplification and enlarged reparative nuclei and prominent nucleoli. (**J** and **K**) In glomerular disease, Ngal was weakly expressed by crescents (**J**) and the proximal tubules of nephrosis (**K**). Scale bars: **A**, **D**, **G**, and **K**, 11 μm; **B**, **C**, **E**, **F**, and **H**–**J**, 5 μm.
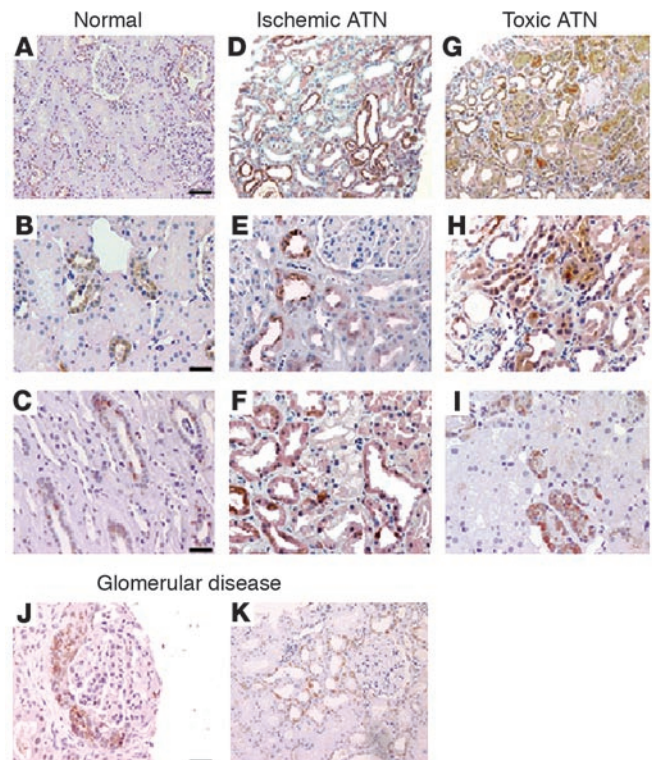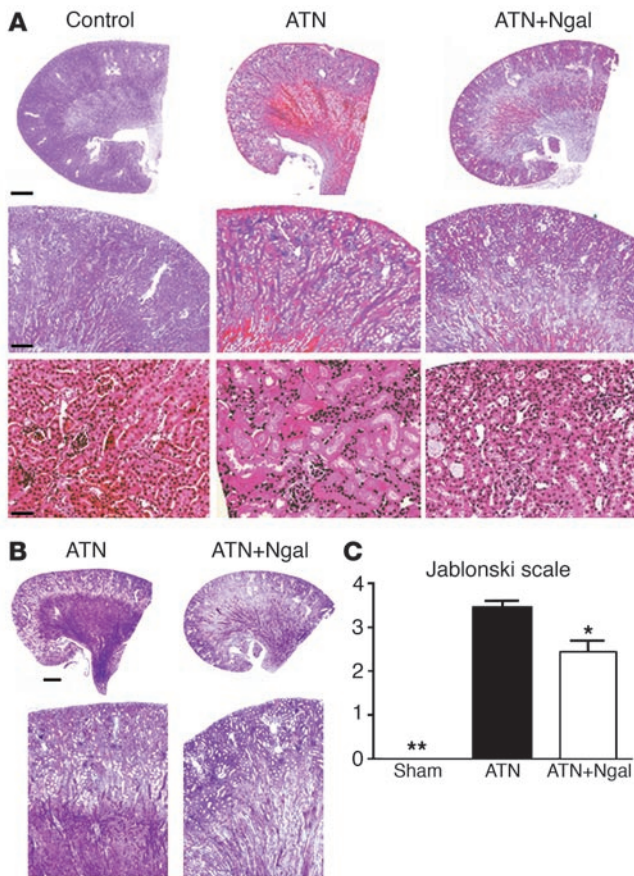
Figure 3
Rescue of mouse ATN by Ngal. (**A**) Holo-Ngal (100 μg) was injected into the peritoneum 15 minutes before renal pedicle cross-clamp and 30 minutes of ischemia. Kidneys were harvested after 24 hours of reperfusion for H&E staining. The ischemic kidneys (ATN) demonstrated loss of tubular nuclei (ATN, bottom) as well as the presence of cortical and medullary intratubular casts (ATN, middle). In contrast, Ngal pretreatment resulted in preservation of cortical tubules (ATN+Ngal, bottom) and reduced cortical-medullary casts (ATN+Ngal, middle). (**B**) PAS staining highlighted the luminal casts in the ischemic kidney (ATN) as well as the rescue of cortical tubules by pretreatment with Ngal (ATN+Ngal). (**C**) Area of proximal convoluted tubular necrosis was evaluated by the Jablonski scale, which demonstrated rescue of the ischemic cortex by Ngal (0: no necrosis; 1: isolated necrotic cells; 2: focal necrosis in inner cortex; 3: diffuse necrosis in inner cortex; 4: necrosis involving whole cortex). *$P < 0.05$, **$P < 0.01$ vs. untreated ischemic kidneys. Scale bars: **A**, top row, 800 μm; middle row, 24 μm; bottom row, 11 μm; **B**, top row, 800 μm; bottom row, 24 μm.

cadherin expression in the ischemic kidney. To test this hypothesis, we first confirmed that, whereas E-cadherin could be detected at a low level in the mouse proximal tubule by immunofluorescence, N-cadherin was specific to the proximal tubule and appeared to be its major cadherin (46) (Figure 4). N-cadherin is known to be processed by caspases, by γ-secretase, and by MMPs, which generate 30- to 40-kDa cytoplasmic fragments that are potentially important signaling molecules that modulate CREB signaling (49). We found that, after ischemia-reperfusion, N-cadherin was degraded to fragments (Figure 4, A and B). In some animals degradation of the protein could be detected within 6 hours of reperfusion, and by 24 hours, both N-cadherin immunofluorescence and expression of the full-length protein were nearly abolished. In contrast, pretreatment with Ngal preserved N-cadherin immunofluorescence, enhanced the expression of full-length N-cadherin, and reduced the appearance of its fragment at 6 hours (in some animals) or 24 hours of reperfusion. E-cadherin, on the other hand, was highly expressed in the distal tubule and collecting duct and was much less affected by ischemia and by Ngal treatment. Similarly, metal-induced nephrotoxic ATN triggered the degradation of N-cadherin but not E-cadherin (50, 51). Perhaps Ngal directly modulates N-cadherin processing, but an indirect effect subsequent to the preservation of tubular morphology by Ngal is more likely.

Because the expression of Ngal correlates with ischemic damage (44), we examined the expression of endogenous Ngal mRNA after treatment with exogenous Ngal protein. We found that treatment of ischemic animals with Ngal (100 μg) reduced the increase in endogenous Ngal RNA by 72% ± 16% ($n = 5$, $P < 0.01$) at 24 hours

of reperfusion as measured by real-time RT-PCR. In addition, the injection of Ngal reduced the appearance of Ngal protein in the kidney by 60% ± 10% (ischemia 73 ± 7 μg/g, Ngal-treated ischemia 29 ± 7 μg/g; $n = 3$ each, $P < 0.01$) as measured by immunoblot.

Because disruption of the proximal cell results in apoptotic cell death, we next examined the effect of Ngal on cell viability (Figure 4, C and D). Twenty-four hours after reperfusion, we counted the percentage of tubules with at least 1 TUNEL⁺ tubular cell. Ischemic kidneys showed that 11.5% ± 0.6% ($n = 4$) of cortical tubules contained TUNEL⁺ cells, but after treatment with Ngal, the percentage of positive tubules fell to 2.9% ± 0.9% ($n = 7$, $P < 0.001$). For comparison, 0.5% ± 0.3% of cortical tubules had TUNEL⁺ cells in sham-operated kidneys. Similarly, we evaluated the uptake of BrdU, a cell proliferation marker. We counted the percentage of cortical tubules with at least 1 BrdU⁺ tubular cell. Twenty-four hours after the insult, ischemic cortical tubules contained rare BrdU⁺ cells (1.9% ± 0.3% of tubules; $n = 3$), while ischemic kidneys pretreated with Ngal had a small but significant increase in positive cells (3.9% ± 0.5% of tubules; $n = 4$, $P < 0.05$). For comparison, 3.7% ± 0.7% of cortical tubules had BrdU⁺ cells in sham-operated kidneys. Hence, rescue by Ngal reduced apoptosis of cortical cells and either stimulated compensatory tubular cell proliferation or else preserved tubular cells with proliferation potential.

Mechanism of rescue from ATN: Ngal targets the proximal tubule. To determine the mechanism by which Ngal protects the proximal tubule from ischemic damage, we first studied the distribution of exogenous Ngal after an i.p. or s.c. injection. Ngal was found in the urine within 10 minutes of injection (10 or 100 μg), suggesting that the protein was rapidly cleared by the kidney (Figure 5). However, only 0.1–0.2% of the injected Ngal was recovered in the urine in the first hour. To better follow trafficking, we used fluorescent conjugates of Ngal. Both fluorescein-labeled and Alexa-labeled Ngal localized to large vesicles in the subapical domain of the cortical proximal tubule (S1 and S2 segments of the nephron) by 1 hour (Figure 6), but not to other segments of the tubule. To determine whether these organelles were lysosomes, we labeled proximal tubular lysosomes with fluorescein-dextran (43 kDa) the day before administration of Alexa 568–Ngal (52). One hour after injection of Ngal, 33% of the Ngal vesicles also contained dextran (Figure 6B). In addition, many of these vesicles costained with the lysosomal marker LAMP1 (data not shown). We obtained similar data by injecting ¹²⁵I-Ngal (Figure 6C), which showed that the full-
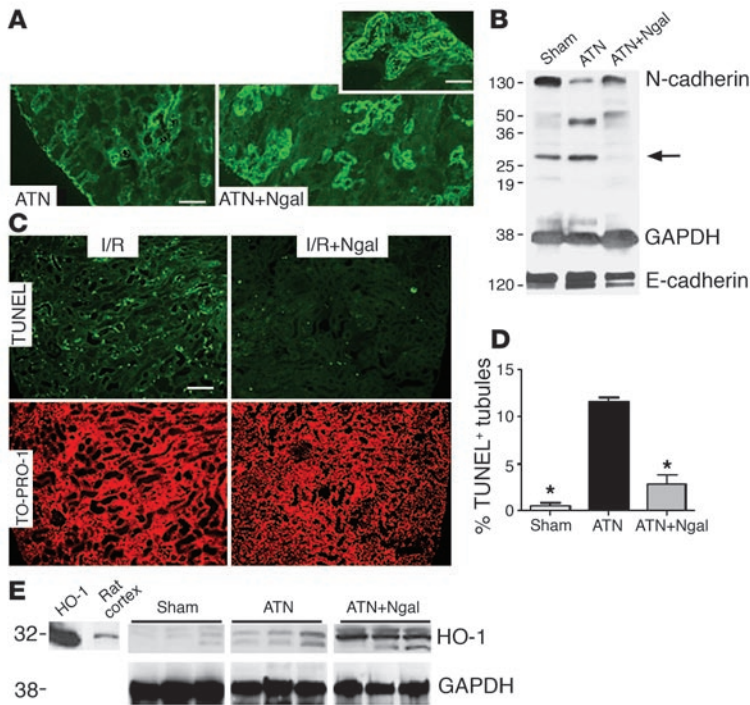
Figure 4
Correlates of ATN. Kidneys were harvested 24 hours after reperfusion. (**A**) N-cadherin staining was nearly abolished by ischemia-reperfusion (ATN), but it predominated apical cell-cell junctions after treatment (100 μg holo-Ngal; ATN+Ngal). (**B**) Full-length N-cadherin (130 kDa) was rescued by Ngal. Note the presence of N-cadherin fragments (28 kDa) in ischemia-reperfusion and sham-treated animals, but their suppression in Ngal-treated animals (arrow). In contrast, there was little change in the level of E-cadherin protein. GAPDH (38 kDa) was the loading control. (**C**) Tubules with TUNEL^{+} apoptotic cells (green fluorescence in ischemia-reperfusion injury; I/R) were reduced by pretreatment with Ngal (I/R+Ngal). TO-PRO-I was the nuclear counterstain (red) for the same field. (**D**) Percentage of tubules containing at least 1 apoptotic nucleus. Ischemia-reperfusion injury increased the number of positive tubules 22-fold, and Ngal reduced the activity fourfold. *$P < 0.001$ vs. I/R. (**E**) Ngal upregulated HO-1 (32 kDa) expression in ischemic kidneys. Kidneys harvested 24 hours after ischemia-reperfusion (ATN) expressed HO-1, but when animals were treated with Ngal, HO-1 expression was enhanced (ATN+Ngal). Purified HO-1 (HO-1) and rat cortex are included for comparison. GAPDH was the loading control. Scale bars: **A** and **C**, 9 μm; **A**, inset, 4.6 μm.

length protein was rapidly cleared from the blood and located in the kidney by the 1-hour time point (for example, the kidney had 13-fold more ^{125}I-Ngal than the liver, per milligram protein). Nearly identical data were previously reported with human Ngal, which rapidly cleared the circulation ($t_{1/2}$ = 10 minutes) and located in the kidney (the kidney had 12-fold more human ^{125}I-Ngal than the liver, per milligram protein) (53). The kidney-localized protein was trichloroacetic acid (TCA) precipitable (70%) and was composed of both full-length Ngal and a specific 14-kDa degradation product. These species persisted and were only slowly lost from the kidney. In contrast, the plasma and, particularly, the urine contained mostly low–molecular weight, TCA-soluble ^{125}I fragments (35% and 20% TCA precipitable, respectively; Figure 6).

These data show that full-length Ngal is rapidly cleared by the proximal tubule, where it traffics to lysosomes and degrades to a 14-kDa fragment. It is likely that the endogenous protein (low levels of serum Ngal) traffics in a similar manner, because there is very little urinary Ngal in normal mouse or human urine, despite the fact that it is freely filtered from the circulation (human: filtered load = 21 ng/ml × GFR, whereas urinary Ngal = 22 ng/ml; mouse: filtered load = 100 ng/ml × GFR, whereas urinary Ngal = 40 ng/ml).

Rescue of the proximal tubule from ATN requires siderophore:Fe. X-ray crystallography and atomic absorption as well as biochemical studies have demonstrated that Ngal cloned in XL1-Blue bacteria contains a siderophore called enterochelin, and that the siderophore carries iron in a 1:1 stoichiometry (41, 42). To determine whether Ngal can deliver iron to the proximal tubule, we prepared [55]Fe-loaded Ngal by incubating iron-free Ngal:enterochelin with [55]Fe at a 1:1 stoichiometry (Ngal:enterochelin:[55]Fe). One hour after injecting this labeled protein (10 μg i.p.), we recovered the majority of [55]Fe in the kidney (55%), but only trace amounts in the plasma (4.3%), urine (0.6%), liver (2.4%,), and spleen (0.2%). To determine the location of the [55]Fe in the kidney, we performed radioautography and found [55]Fe in the proximal

tubule, particularly along the apical surface, beneath the brush border (Figure 6E; Table 1). In contrast, [55]Fe was not found in the medulla (Figure 6D). These data show that both the Ngal protein and its ligand, iron, can be captured by the proximal tubule when the complex is given exogenously. It should be noted that the distribution of Ngal:enterochelin:[55]Fe was quite different from the distribution of non–protein-bound [55]Fe citrate (where kidney recovery was only 2.8%; ref. 54).

To determine the role of iron delivery in renal protection, we compared iron-loaded and iron-free Ngal. Ngal cloned in XL1-Blue contains enterochelin and is iron loaded, and this form of Ngal protected the kidney (holo-Ngal; Figure 7A). In contrast, Ngal cloned in BL21 bacteria does not contain enterochelin and is not iron loaded (apo-Ngal) (41), and it only partially protected the kidney; this suggests that the siderophore:Fe was the critical factor (Figure 7A). To test this hypothesis further, we
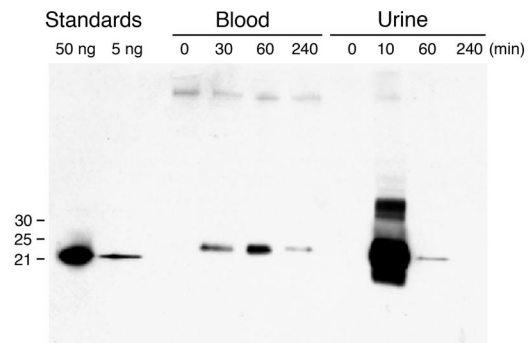
Figure 5
Clearance of Ngal. Ngal (100 μg) was introduced into the peritoneum, and serum (5 μl) and urine (1 μl) samples collected after the time indicated were analyzed by immunoblot.

Table 1
Subcellular localization of iron in the kidney cortex 1 hour after
i.p. injection of Ngal:siderophore:^{55}Fe complex

Location	Silver grains[A] (% total)	Area[B] (% point count)	S/A ratio[C]	χ^2
Lumen	26.46	18.49	1.43	3.43
Apical membrane	12.91	5.84	2.21	8.54
Cytosol	48.98	48.81	1.00	0.00062
Nucleus	4.02	7.17	0.56	1.39
Basal membrane	3.81	6.41	0.59	1.06
Interstitium	3.71	12.20	0.30	5.91
Glomerular tuft	0.13	1.16	0.11	0.91
			$\chi^2 = 21.2, P = 0.0017$	

[A]Total silver grains, 2,601; [B]total point count, 999; [C]percent grains/
percent point count.

reconstituted apo-Ngal (from BL21) with iron-saturated entero-
chelin (red protein, Figure 7B). In contrast to apo-Ngal, Ngal:
enterochelin:Fe enhanced the protection of the kidney and blunt-
ed the rise in serum creatinine. These data suggest that Ngal pro-
vides protection against ischemia by delivering siderophore:Fe
to proximal tubules.

Because the iron-loaded form of Ngal contains 2 ligands (iron
and enterochelin), we wished to identify the effective molecule
by designing an experiment whereby Ngal:enterochelin could be
delivered to the kidney without iron. However, we realized that
iron-free Ngal:enterochelin is not likely to arrive in the proximal

tubule without iron, because of the great avidity of the siderophore
(10^{-49} M) (41), which allows it to strip iron from transferrin (55).
Furthermore, when we loaded a mouse with ^{55}FeCl and then intro-
duced iron-free Ngal:enterochelin (100 μg/0.05 ml PBS) 5 and 35
minutes after the dose of iron, we found that the recovery of ^{55}Fe at
65 minutes increased 3-fold (percentage initial dose) from the kid-
ney and urine and decreased threefold from the liver and spleen,
compared with that in mice receiving PBS. These data indicate
that Ngal:enterochelin and Ngal:enterochelin:Fe are equivalent
after introduction in vivo, supporting the view that Ngal:sidero-
phore acts as an iron delivery protein. Indeed, we found that the
iron-free form of Ngal:enterochelin (white protein, Figure 7B) was
as effective in vivo as the iron-loaded form (Figure 7A).

To test the role of Ngal ligands further, we prepared gallium-
complexed Ngal. Because gallium is a metal^{+3} that occupies iron-
binding sites with high affinity, including enterochelin, but can-
not undergo redox reactions typical of iron, gallium acts as an
iron antagonist. In contrast to the iron complex, mice treated 15
minutes before ischemia with Ngal:enterochelin:gallium were not
protected (creatinine 3.17 ± 0.1 mg/dl; $n = 4$; Figure 7A). These data
suggest that not only does Ngal transport iron, but iron transport
is necessary for its activity.

It should be noted that protein delivery to the proximal tubule
itself is not likely to be the mechanism of protection, because a
second lipocalin, retinol-loaded retinol-binding protein (RBP),
which is also captured by the proximal tubule and degraded in
lysosomes, was ineffective (Figure 7A). Furthermore, free entero-
chelin and the iron chelator DFO were also ineffective compared
with Ngal:enterochelin, even at higher molar doses.

Figure 6
Clearance of Ngal by the proximal tubule. (**A**)
Fluorescent Ngal (100 μg, labeled with Alexa
568) was introduced into the peritoneum,
and after 1 hour the kidney was harvested
and sectioned. Fluorescent Ngal was local-
ized to large vesicles in the proximal tubule
(bottom panel) but not in the glomerulus (G)
or medulla (small top panels). Uncoupled
dye did not label the kidney (Alexa 568
only). (**B**) Alexa 568–Ngal colocalized with
FITC-dextran in S1 and S2 segments of the
proximal tubule. Dextran was introduced into
the animal 1 day before the Ngal injection in
order to label lysosomes. (**C**) ^{125}I-Ngal was
introduced into mice, and the samples were
assayed by SDS-PAGE. Lanes were load-
ed with 1,000 cpm each. The lane marked
"Ngal" shows the initial preparation of
^{125}I-Ngal. Subsequent lanes of urine or blood
show loss of signal, suggesting degradation
to small fragments. However, full-length Ngal
and a 14-kDa fragment of Ngal were found
in the kidney 1 and 5 hours after injection.
(**D** and **E**) Radioautograph of kidney 1 hour
after i.p. injection of ^{55}Fe-loaded Ngal:sid-
erophore. Radioactivity was not found in the
medulla (**D**). In contrast, radioactive decay
was found in the cortex and was associated
with the apical zones of proximal tubule cells
(**E**). Original magnification, **A** and **B**, ×40; **A**,
inset, ×10. Scale bar: **D** and **E**, 2 μm.
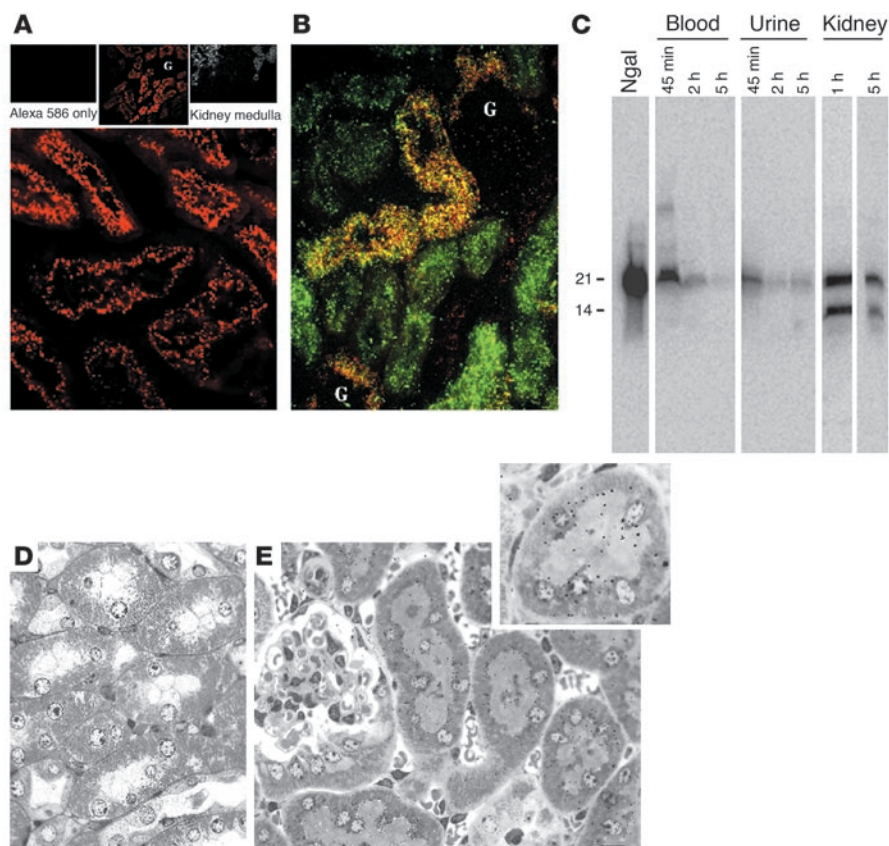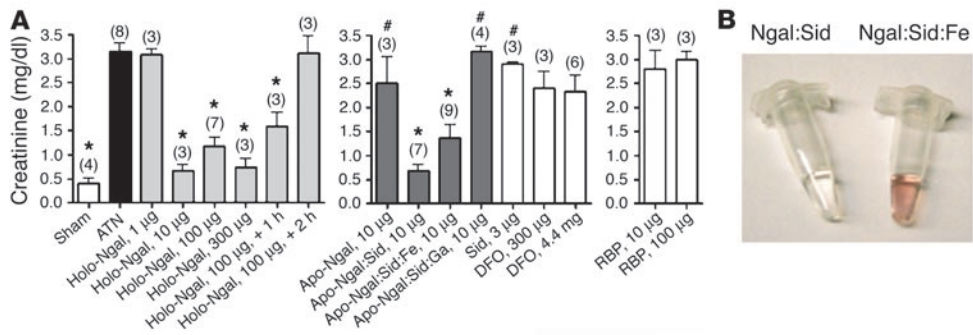
Figure 7
Rescue of ATN by Ngal. (**A**) Plasma creatinine in mice subjected to 30 minutes of ischemia followed by 24 hours of reperfusion. The first panel shows that holo-Ngal (≥10 μg) from XL1-Blue bacteria (containing siderophore and iron) rescued renal function when introduced 15 minutes before ischemia or within 1 hour after ischemia (+ 1 h). However, Ngal was ineffective when administered later (+ 2 h). The second panel shows that apo-Ngal from BL21 bacteria (siderophore free) was minimally active, but that, when loaded with a siderophore (enterochelin), the protein was protective: both iron-free (apo-Ngal:Sid) and iron-loaded siderophores (apo-Ngal:Sid:Fe) had a protective effect. In comparison, the gallium-loaded complex (apo-Ngal:Sid:gallium) was ineffective, as was a single dose of the iron chelator DFO or the free siderophore (Sid). Retinol-binding protein (RBP), a lipocalin that is also filtered and reabsorbed by the proximal tubule, was ineffective. *$P < 0.001$ vs. ATN. #$P < 0.01$ vs. apo-Ngal:Sid (10 μg). The numbers in parentheses show the number of animals analyzed. (**B**) Preparations of Ngal. Ngal:Sid contains enterochelin, but not iron. Ngal:Sid:Fe contains enterochelin and iron.
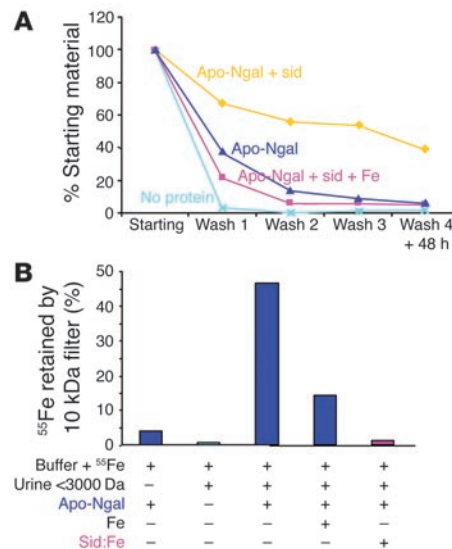
Ngal upregulates HO-1 in ATN. A number of studies have identified HO-1 as a critical regulator of the proximal tubule viability in renal ischemia. HO is necessary for recovery from ATN (56–58), and its level of expression is directly correlated with the rescue of tissue damage. We found that ischemia-reperfusion enhanced the expression of HO-1, but when mice were treated with Ngal (10–100 μg), the enzyme was further upregulated 5- to 10-fold by 24 hours after reperfusion (Figure 4E). To determine whether holo-Ngal itself, or holo-Ngal in the setting of renal ischemia, induced HO-1, we injected normal mice with increasing doses of Ngal and found upregulation of the protein. However, the expression of HO-1 after Ngal injection was much less than in Ngal-treated ischemic kidneys, which indicates that Ngal synergizes with other activators of HO-1.

To determine whether HO-1 activity was required for Ngal activity, we used the well-known inhibitor zinc protoporphyrin IX (see Methods). We found that, while Ngal:enterochelin:Fe (40 μg) protected the kidney from ischemia-reperfusion damage (creatinine = 0.91 ± 0.16 mg/dl; $n = 3$), injection of the HO inhibitor blocked the effect (creatinine = 2.74 ± 0.45 mg/dl; $n = 5$, $P < 0.05$). Hence, HO activity is required for Ngal-mediated protection.

Figure 8
Iron-binding cofactor in urine. (**A**) Buffer was mixed with ^{55}Fe (No protein, light blue) and with apo-Ngal (dark blue), apo-Ngal plus siderophore (yellow), or apo-Ngal plus siderophore plus unlabeled iron (pink). The samples were then washed 3 times on a 10-kDa filter, and small aliquots were measured for retention of radioactivity (Washes 1–3). After 48 hours at 4°C the samples were washed again (Wash 4 + 48 h). Note the retention of ^{55}Fe by apo-Ngal plus siderophore but not by apo-Ngal alone or apo-Ngal ligated by the iron-saturated siderophore, which demonstrates that an unsaturated siderophore is required for retention of ^{55}Fe by Ngal. ^{55}Fe binding to apo-Ngal plus siderophore was stable for 48 hours. (**B**) Urine (<3,000 Da) was mixed with ^{55}Fe and with apo-Ngal, as indicated, and then washed 3 times on a 10-kDa filter. While urine (<3,000 Da) or apo-Ngal in buffer did not retain ^{55}Fe on a 10-kDa filter, apo-Ngal plus urine retained ^{55}Fe. ^{55}Fe retention was blocked by the addition of excess iron citrate (Fe) or of iron-saturated enterochelin (Sid:Fe).

A urine siderophore? The actions of endogenous Ngal in vivo might differ from its pharmacological effects, because the critical siderophore is a bacterial product. Low–molecular weight factors that transport iron, however, have been suggested by a variety of studies (59–61). These molecules may include citrate and related compounds, but also iron-transporting activities that have a molecular weight in the range of 1,000 Da. To determine whether a cofactor for Ngal is present in the urine, we mixed apo-Ngal with urine samples from normal mice. While neither apo-Ngal diluted in Tris buffer (Figure 8A) nor the low–molecular weight components of the urine (<3,000 Da) trapped ^{55}Fe above a 10,000-Da cutoff filter (Figure 8B), incubation of Ngal with urine (<3,000 Da) permitted the retention of ^{55}Fe. The capture of iron by Ngal was inhibited by 1,000-fold unlabeled iron citrate, and more powerfully by a 50-fold concentration of the iron-saturated enterochelin (Figure 8B, Sid:Fe). The capture of iron was satu-

rable by increasing doses of urine. These findings suggest that mouse urine contains a low–molecular weight cofactor that permits Ngal-iron interactions. Because the endogenous factor is competitive with the bacterial siderophore, which binds the Ngal calyx with high affinity (0.4 nM) (41), it appears that both bacterial and mammalian factors occupy the same binding pocket of the lipocalin. However, the chemical structure of the mammalian factor likely differs from that of enterochelin, since, whereas the bacterial siderophore was extractable in ethyl acetate, the mammalian factor was more polar and remained in the aqueous phase. Unlike simple salts, the factor was also soluble in methanol and could be eluted from silica resin with methanol.

Discussion

We showed that Ngal is a renal lipocalin that is highly accumulated in the human and mouse proximal tubule during ATN. The synthesis of Ngal protein is markedly upregulated within hours of ischemia-reperfusion injury (44). However, if Ngal is presented before, or in the early stages of, cell damage, there is rescue of N-cadherin (a pathway not previously described in renal disease), enhanced expression of HO-1 (a protective enzyme), and the suppression of endogenous Ngal (a marker of epithelial damage) and blunting of cell death. The preservation of renal function was due not to Ngal itself, but to a siderophore bound in the Ngal calyx. While this cofactor is a bacterial product obtained from cloning of the protein in bacteria, surely a serendipitous finding, we suggest that mouse urine contains an equivalent factor. Hence Ngal is a siderophore delivery protein for the proximal tubule, and this study is one of the first to use a bacterial siderophore in vivo (62).

It is currently unknown how the proximal tubule captures Ngal. Indeed, an unambiguous identification of receptors for most lipocalins is still lacking. Perhaps megalin, which is necessary for reclamation of RBP, is also the Ngal receptor (63). In fact, knockout of megalin leads to the appearance of Ngal in the urine (E.I. Christensen and T. Willnow, personal communication; as shown in Supplemental Figure; supplemental material available online with this article; doi:10.1172/JCI200523056DS1), but these animals were also, unexpectedly, found to have much higher levels of Ngal message in the kidney (64), which suggests that urinary Ngal might have derived from local synthesis rather than a failure to capture the filtered load. Despite this ambiguity, we believe that Ngal is similar to other lipocalins, such as RBP and the α-2u-globulin lipocalin (65), that enter the cell by a megalin pathway and traffic to lysosomes (dextran+, LAMP1+) for degradation. These data contrast with the trafficking of Ngal in cell lines that do not express megalin (such as embryonic metanephric mesenchymal cells) and where the protein escapes degradation (39). Similarly, transferrin is degraded by a megalin-cubilin–based pathway in the proximal tubule (66), whereas the protein recycles after endocytosis in cell lines. Hence it is reasonable to propose that after filtration, Ngal is captured by megalin, is degraded by the proximal tubule, and is not recycled. This hypothesis is supported by the observation that full-length Ngal does not reappear in the blood at delayed time points after injection.

Members of the lipocalin superfamily are transport proteins for low–molecular weight hydrophobic chemicals. Well-known ligands include pheromones (67) and fatty acids, which bind α-2u-globulins and the major urinary proteins, and retinoids, which bind RBP (68). Less-known ligands include iron and its cofactors, but nitrophorins provide a precedent. Insect nitropho-

rins, for example, contain iron-loaded heme groups that transport NO to the site of a bite (69). α₁-Microglobulin (70) binds heme and produces the yellow-brown pigment in the urine. A wide range of siderophores were recently demonstrated to bind tear lipocalin (71). Ngal's ligand is a bacterial siderophore (enterochelin) that can transfer iron to cells or chelate iron from cells. We showed this in vitro by monitoring changes in the level of expression of genes carrying iron-responsive elements (IREs), such as ferritin and transferrin receptor 1 (39), and more sensitively by monitoring changes in the level of expression of reporter constructs that contain IREs coupled to fluorescent proteins (43). In contrast to these responses, we were unable to show activation or suppression of a variety of signaling pathways measured with 18 phospho-antibodies (including those for Raf, MEK, ERK, p38, JNK, and PKC isoforms) in developing kidneys treated with Ngal for 20 minutes or for 1 hour. Hence Ngal is a siderophore:Fe transport and delivery protein, and we suggest that this is its protective mechanism. Indeed, most of the Ngal protein (^{125}I-Ngal and fluorescent) and its bound [55]Fe were delivered to lysosomes in the S1 and S2 segments of the proximal tubule, but neither free iron (54) nor free siderophore (which binds serum albumin; ref. 72) could be delivered. It seems likely that siderophore:Fe is transferred to the cytoplasm from the complex, since the protein is degraded in the proximal tubule.

We previously showed that induction of epithelia from mesenchyme was enhanced by loading of Ngal with enterochelin and with iron (43). In the current work we again show that the Ngal:siderophore complex, rather than apo-Ngal, is the active factor, implicating the ligands of Ngal, rather than the carrier protein itself. We argue here that siderophore:Fe delivery rather than iron chelation is the mechanism of action of Ngal. First, iron-free Ngal:siderophore probably obtains iron during transit from the peritoneum to the proximal tubule, because enterochelin is so avid for iron ($K_d = 10^{-49}$ M) (42). Indeed, iron-free enterochelin can strip iron from transferrin (55), and iron-free Ngal:siderophore redirects [55]Fe from the spleen and the liver (54) and produces a threefold increase in kidney and urinary [55]Fe contents after injection of iron-free Ngal:siderophore and [55]Fe in vivo. Because Ngal is cleared by glomerular filtration, the shift in [55]Fe to the kidney and to the urine indicates that iron-free Ngal became iron loaded during transit. Hence iron-loaded and iron-unloaded Ngal:siderophore delivers iron to the proximal tubule.

We also argue that iron chelation is not like the mechanism of protection by Ngal:siderophore:Fe, because in order to act as an iron chelator, iron would first have to dissociate from enterochelin, which, at least in solution, occurs too slowly to be relevant (Figure 8) and, in any case, would not produce a net loss of iron. Moreover, if enterochelin were liberated from Ngal after endocytosis, it would degrade both spontaneously and by the action of esterases (73), and the decay products probably cannot cause a net loss of iron (74). Third, while Ngal:siderophore:Fe was protective, the gallium homologue was inactive, despite the fact that enterochelin:gallium derivatives (75) and Ngal:enterochelin:gallium traffic to the kidney and despite the fact that gallium might even exchange for iron in the siderophore complex (76). Gallium DFO can even be an effective scavenger of catalytic iron (77) and reduce reactive oxygen species. Hence Ngal:enterochelin:gallium is ineffective not because it can never chelate iron, but because it does not deliver the siderophore:Fe complex. Fourth, the pharmacology of the iron chelators differs from the actions of Ngal:siderophore. For exam-

ple, in most studies, desferri-DFO (16) is continuously infused and single doses, unlike Ngal, are not protective. In fact, while DFO is mostly excreted in the urine, Ngal is recovered by the proximal tubule, which indicates that the Ngal:siderophore is more likely to transfer iron to proximal tubule cells rather than remove iron from these cells. Similarly, iron chelation by apo-transferrin reduced azotemia in vivo, but unlike Ngal, it did not mitigate apoptosis (18). Desferri-exochelin (20), another type of apo-siderophore, protected the heart from ischemic damage in an in vitro model of coronary artery ligation (20), but this has not been shown by systemic infusion, where the siderophore would be exposed to many sources of iron. Hence while many studies unequivocally demonstrate that iron chelation ameliorates ischemia-reperfusion damage, and that the lipophilicity of siderophores allows tissue penetration, and perhaps access to membrane-associated iron that generates hydroxyl radicals (6, 20), siderophore:Fe donation by Ngal, rather than iron chelation, explains the data.

The delivery of iron could be protective and enhance cell repair for a number of reasons. Low doses of iron or heme, or other iron donors (78, 79), induce HO-1 (56, 80). This enzyme is both necessary and sufficient in a dose-dependent fashion to protect epithelia (refs. 56, 81, 82; reviewed in 83) from ischemia (57, 58) and nephrotoxicity (84). In fact, the enzyme is specifically induced in the proximal tubule (85) by a large number of insults (56), and it prevents iron overload in both mouse (86) and human (85) proximal tubules. HO-1 is thought to protect cells by limiting uptake and enhancing the release of iron and thus to reduce the cell content of non–ferritin-bound iron (31). In addition, it synthesizes antioxidant biliverdin and CO and can induce p21 (reviewed in refs. 79, 87, 88). Treatment with Ngal:siderophore resulted in low levels of expression of HO-1 in normal proximal tubules, but markedly enhanced expression of HO-1 in the ischemic tissues. We speculate that this induction is the critical pathway by which Ngal protects the proximal tubule, an idea supported by loss of Ngal activity after introduction of the HO inhibitor. However, in addition to HO-1 there are many other iron regulatory pathways (ferritin) and non-iron pathways (cell replication) that Ngal may stimulate by delivering iron. For example, iron is necessary for the R2 subunit of ribonuclease reductase, the enzyme that synthesizes DNA (89); it enhances the expression of many cyclin genes (90) and stress-related proteins (91); and it inhibits apoptosis mediated by p38 MAPK phosphorylation (92) and NIP3 (93). Last, it is even possible that enterochelin:Fe or its degradation products may scavenge free radicals.

A model of the postischemic kidney might focus on the idea of "cell shift," rather than on the pathologic consequences of catalytic iron alone. Transport of iron into viable proximal tubule cells could supply iron for cell proliferation as well as activate the disposal of excess iron by HO-1 (31), whereas loss of iron from the cell is proapoptotic. Chelation of extracellular iron, on the other hand, would reduce free radical formation and hence provide protection from ischemic damage by a different mechanism at a later point in the disease process. To test these hypotheses it will be necessary to detect the effect of the Ngal complex on iron levels in the proximal tubular cells in vivo (available cell lines have little uptake of Ngal) and to distinguish between damaged and viable cells. Perhaps expression of our IRE–yellow fluorescent protein construct (43) in the proximal tubules of animals could provide real-time monitoring of iron in the first hours after Ngal is captured by these cells and over the course of ischemic disease.

Bacterial siderophore–mediated rescue of the proximal tubule raises the fundamental question of whether mammalian-expressed Ngal has the same type of ligand as the recombinant protein. Early studies from the laboratories of J.A. Fernandez-Pol (59) and A. Cerami (60) suggested that low–molecular weight iron carriers were expressed by mammalian cells, but their identification was not established, nor were carrier proteins like Ngal implicated in their traffic. However, we found a factor in the mouse urine that was competitive with the bacterial siderophore. Hence if such a factor was available in the ischemic kidney, it would suggest that Ngal mediates autocrine or paracrine iron trafficking. These hypotheses might be validated, first, by protection of the kidney with Ngal loaded with the mammalian factor, rather than the bacterial siderophore, and, second, by demonstration that ischemic damage is prolonged in mice or humans with defective expression of Ngal or its putative cofactor. Creation of Ngal knockout mice, and knockouts specific to kidney Ngal, would be a first step.

Lastly, because Ngal has been suggested to regulate leukocytes by inducing apoptosis after receptor-mediated signaling (94), it remains possible that Ngal is a bifunctional molecule and has actions other than siderophore transport. Perhaps endogenously expressed Ngal, which peaks hours after ischemia-reperfusion injury, might reduce the population of invading leukocytes and, conversely, Ngal-deleted animals have a greater burden of these cells. However, rather than a proapoptotic action, we could only document that Ngal reduced, rather than increased, TUNEL staining in the ischemic kidney. Most importantly, it is improbable that exogenous Ngal regulates populations of leukocytes, because it was effective before or in the first hours of ischemia-reperfusion, and its actions depend on its siderophore:Fe ligand.

In sum, ischemia-reperfusion has been shown to change the activity of a few components of iron metabolism. We demonstrate that a siderophore-binding protein is highly overexpressed in these diseases and that a single systemic administration of holoprotein, the iron-transporting form of Ngal, mitigates injury. While liver cells may also accumulate iron in the initial phases of ischemia reoxygenation by upregulating the transferrin receptor, the proximal tubule may have special mechanisms to acquire iron, because these cells do not express transferrin receptors (66). In addition to the previously described apical megalin-transferrin (66), the current data demonstrate an apical Ngal-iron pathway. Our data are applicable to the human, where we found Ngal to be highly expressed in renal diseases.

Methods

Patients. We analyzed healthy volunteers and patients diagnosed with either acute or chronic renal failure. Acute renal failure was diagnosed by a doubling of the serum creatinine in less than 5 days. The definition of chronic renal failure was a serum creatinine greater than 2 mg/dl, but unchanged during the prior 2 months. The presumed etiology of acute renal failure included sepsis, which was defined by the presence of the following criteria: (a) positive blood cultures or evidence of local infection in the lung, skin, or urinary tract, and (b) fever or an elevated white blood cell count. Some of these patients required blood pressure support. Other etiologies of ATN included hypotension due to bleeding or heart failure, nephrotoxins, and post-transplantation ischemia. The presumed etiologies of chronic renal failure included obstructive uropathy, chronic interstitial nephritis, and diabetes. Samples of blood and urine were collected from patients evaluated at Columbia University Medical Center and at Kyoto University Hospital with approval of both Institutional Review Boards and then analyzed in a blinded fashion.

Measurement of Ngal. An anti–mouse Ngal polyclonal antibody was raised in rabbits, purified on a column of Sepharose 4 Fast Flow beads (Amersham Biosciences) coupled to recombinant mouse Ngal (see below), and then eluted at pH 2.5. Monoclonal anti–human Ngal (AntibodyShop A/S; 1:1,000) was also used to detect Ngal. Human Ngal was better recognized by the mAb, while mouse Ngal was recognized only by the affinity-purified polyclonal antibody.

Human blood samples were initially collected in citrate, EDTA, or heparin, but all of these preparations showed similar Ngal immunoreactivity, and we chose to study human serum and mouse plasma. The samples were centrifuged through a 100-kDa cutoff filter (Amicon YM-100; Millipore Corp.), and the flow-through was used for immunoblot. In patients undergoing hemodialysis, samples were taken immediately before dialysis. Fresh urine samples were centrifuged at low speed to remove debris and then used without further concentration.

Pathologic specimens. Pathologic specimens included ischemic ATN (10 cases), toxic ATN (11 cases: 5 caused by antibiotics, 2 by zoledronate [ref. 95], 1 by carboplatinum, 2 by nonsteroidal anti-inflammatory agents, and 1 by hemoglobinuria), and glomerulopathies (10 cases, including diabetic nephropathy, anti–glomerular basement membrane disease, pauci-immune crescentic glomerulonephritis, IgA nephropathy, minimal-change disease, and focal segmental glomerulosclerosis), and also normal kidneys (3 cases). Formalin-fixed, paraffin-embedded tissues were sectioned (5 μm) and subjected to antigen retrieval using microwave in a citrate buffer (pH 6.0) for 30 minutes. Endogenous peroxidase was blocked with 5% H_2O_2 for 30 minutes, followed by blocking in 10% goat serum/1% BSA. Affinity-purified anti–mouse Ngal (0.4 μg/ml) was applied overnight at 4°C, followed by biotinylated goat anti-rabbit IgG (1:100; Vector Laboratories Inc.) and avidin-HRP, each for 30 minutes. Slides were developed with DAB/0.3% H_2O_2 for 2.5 minutes and counterstained with hematoxylin. Nonimmune rabbit IgG (0.4 μg/ml; Vector Laboratories Inc.) was used as a control.

Recombinant Ngal. Recombinant human and mouse glutathione-S-transferase–Ngal was expressed in BL21 or XL1-Blue strains of *E. coli* (Stratagene) (39, 41, 96) with additional ferric sulfate (50 μM; Sigma-Aldrich). Ngal was isolated using Glutathione Sepharose 4B beads (Amersham Biosciences), eluted by thrombin cleavage (Sigma-Aldrich), and then further purified by gel filtration (Superdex 75, SMART system; Amersham Biosciences) and examined by Coomassie gels (Bio-Rad Laboratories Inc.). BL21-derived Ngal was loaded with iron-free or iron-saturated enterochelin (0.7 kDa; EMC Microcollections GmbH) using a 5-fold molar excess. Unbound siderophore was removed by washing in a Microcon YM-10 centrifugal filter (Millipore Corp.) with PBS. To produce ^{55}Fe- or gallium-loaded Ngal, we incubated the iron-free Ngal:enterochelin complex with equimolar ^{55}Fe or gallium in 150 mM NaCl/20 mM HEPES (pH 7.4), and the complex was washed 3 times on a 10-kDa filter. Iodobeads (Pierce) were used to label Ngal with ^{125}I, and unincorporated ^{125}I was removed by gel filtration (PD-10 column, Amersham Biosciences) followed by extensive dialysis (7-kDa cutoff membrane; Pierce) against PBS. Alexa 568 and FITC (Molecular Probes) were coupled to Ngal, according to the manufacturer's instructions, and then extensively dialyzed. Protein was measured by Coomassie gels in comparison with BSA standard.

Ngal trafficking. To detect Ngal delivery to the kidney, recombinant Ngal (10 or 100 μg), Alexa 568–Ngal (100 μg), ^{125}I-Ngal (10 μg, 2 × 10^6 cpm), or Ngal:enterochelin:^{55}Fe (10 μg, 1 × 10^6 cpm) was injected into the peritoneum, and the blood, urine, kidney, liver, and spleen were obtained. Ngal was detected by immunoblot. Alexa 568–Ngal was detected by confocal microscopy (LSM META detector, Carl Zeiss), and Ngal-mediated iron trafficking was detected by scintillation counter and by light microscopic radioautography of Epon-embedded kidneys. Slides were exposed to emulsion (Polysciences Inc.) for 1 week and then developed with MICRODOL (Eastman

Kodak Co.) and counterstained with toluidine blue. To detect lysosomes in the proximal tubule, mice were injected with fluorescein-dextran (43 kDa, 0.5 mg; Sigma-Aldrich) 24 hours before Alexa 568–Ngal (100 μg) was introduced. LAMP1 (Santa Cruz Biotechnology Inc.) was detected in cryostat sections of kidneys fixed in 4% paraformaldehyde.

Mouse ATN. Use of mice was approved by the Institutional Animal Care and Use Committee of Columbia University. Male C57BL/6 mice (20–25 g; Charles River Laboratories Inc.) were anesthetized with i.p. pentobarbital (50 mg/kg) and placed on a heating pad under a warming light to maintain 37°C core body temperature. Kidneys were exposed through an abdominal section, and the right kidney was removed or its vascular pedicle and ureter ligated. The vascular pedicle of the left kidney was clamped by a micro-aneurysm clip (Kent Scientific Corp.) for 30 minutes after right nephrectomy. This period of ischemia generated reproducible renal injury, but it minimized mortality (97). In our series, we had 11% mortality in untreated animals, but Ngal:siderophore or Ngal:siderophore:Fe treatment reduced mortality to 2%. During surgery, PBS (0.5 ml) was used to dampen the peritoneum, and the animal was then closed with 5-0 nylon. Ngal, retinol-loaded RBP (a kind gift of W.S. Blaner, Columbia University) (98), enterochelin, or DFO mesylate (Sigma-Aldrich) was injected into the peritoneum or s.c. 15 minutes before ischemia or 1–2 hours after reperfusion. These substances were diluted in 0.05 ml of PBS, whereas control animals received 0.05 ml of PBS alone. The HO inhibitor zinc protoporphyrin IX (Sigma-Aldrich) (99) and vehicle (both 10 μmol/kg dissolved in 2 mM NaOH, neutralized with equimolar HCl, and then diluted to 0.05 ml with PBS) were introduced into the peritoneum 20 minutes before ischemia, and also 4 hours after reperfusion.

After 6 or 24 hours of reperfusion, heparinized plasma, urine, and kidney were obtained to measure Ngal (polyclonal, 1:500), HO-1 (Stress-Gen Biotechnologies Corp.; 1:2,000), E-cadherin (BD Transduction Laboratories; BD Biosciences − Pharmingen; 1:2,000), N-cadherin (BD Transduction Laboratories; BD Biosciences − Pharmingen; 1:3,000), and GAPDH (Chemicon International Inc.; 1:3,000) using immunoblots. Plasma was also used for creatinine and blood urea nitrogen colorimetric assays (Sigma-Aldrich) (100). Sagittal sections of the kidneys were fixed in 4% formalin or were snap-frozen for mRNA and protein analysis. Paraffin-embedded sections (5 μm) were stained with H&E or by an in situ kit (fluorescein-TUNEL; Roche Applied Science) for apoptotic nuclei or total nuclei (TO-PRO-l; Molecular Probes). For cell proliferation, BrdU (50 mg/kg) was injected into the peritoneum 1 hour before sacrifice, and cryostat sections were stained with anti-BrdU (Roche Applied Science) according to the manufacturer's instructions.

Real-time RT-PCR. Total RNA was extracted from mouse kidneys using RNeasy Mini Kit (QIAGEN Inc.) with on-column DNase digestion according to the manufacturer's instructions. The cDNA template was synthesized using Omniscript Reverse Transcriptase and oligo-dT primer (QIAGEN Inc.). The PCR reaction was carried out using iQ SYBR Green Supermix and MyiQ single-color real-time PCR detection system (Bio-Rad Laboratories Inc.) with incubation times of 2 minutes at 95°C, followed by 40 cycles of 30 seconds at 95°C and 30 seconds at 60°C. Specificity of the amplification was checked by melting curve analysis and by agarose gel electrophoresis. Primer sequences for mouse Ngal mRNA (GenBank NM_008491) were CTCAGAACTTGATCCCTGCC (forward primer, positions 93–112) and TCCTTGAGGCCCAGAGACTT (reverse, 576–557). Sequences for mouse β-actin mRNA (GenBank X03672) were CTAAGGCCAACCGTGAAAAG (forward, 415–434) and TCTCAGCTGTGGTGGTGAAG (reverse, 696–677). Each plate included a dilution series of standard samples, which were used to quantify Ngal mRNA. Values were normalized for β-actin mRNA.

Iron-binding cofactor. Cofactor-dependent iron binding to Ngal was measured in 150 mM NaCl/20 mM Tris (pH 7.4) buffer (100 μl) with apo-

Ngal (10 μM), ^{55}Fe (1 μM), and a low–molecular weight fraction (<3,000 Da) of mouse urine (0–30 μl). The urine fraction was obtained by passing of fresh urine sequentially through 10-kDa and 3-kDa membranes (Amicon YM-10 and YM-3; Millipore Corp.). After 60 minutes at room temperature, the mixture was then washed 3 times on a 10-kDa membrane (Amicon YM-10; Millipore Corp.). Ngal loaded with iron-free enterochelin (rather than apo-Ngal) served as a positive control for iron capture. Ferric citrate (1 mM) or iron-loaded enterochelin (siderophore:Fe, 50 μM) was used as a competitor of ^{55}Fe binding.

Statistics. The data were expressed as means ± SEM and analyzed by 1-way ANOVA with Bonferroni's post hoc test for comparison across groups. Ngal levels in humans were log-transformed for statistical analysis. The Jablonski score of kidney damage was analyzed by the Kruskal-Wallis test with Dunn's post hoc test.

1. Lieberthal, W., and Nigam, S.K. 2000. Acute renal failure. II. Experimental models of acute renal failure: imperfect but indispensable. *Am. J. Physiol. Renal Physiol.* **278**:F1–F12.
2. Bonventre, J.V. 2003. Dedifferentiation and proliferation of surviving epithelial cells in acute renal failure. *J. Am. Soc. Nephrol.* **14**(Suppl. 1):S55–S61.
3. Schrier, R.W., Wang, W., Poole, B., and Mitra, A. 2004. Acute renal failure: definitions, diagnosis, pathogenesis, and therapy. *J. Clin. Invest.* **114**:5–14. doi:10.1172/JCI200422353.
4. Halliwell, B., and Gutteridge, J.M. 1990. Role of free radicals and catalytic metal ions in human disease: an overview. *Methods Enzymol.* **186**:1–85.
5. McCord, J.M. 1985. Oxygen-derived free radicals in postischemic tissue injury. *N. Engl. J. Med.* **312**:159–163.
6. Meneghini, R. 1997. Iron homeostasis, oxidative stress, and DNA damage. *Free Radic. Biol. Med.* **23**:783–792.
7. Baliga, R., Zhang, Z., Baliga, M., and Shah, S.V. 1996. Evidence for cytochrome P-450 as a source of catalytic iron in myoglobinuric acute renal failure. *Kidney Int.* **49**:362–369.
8. Baliga, R., Zhang, Z., Baliga, M., Ueda, N., and Shah, S.V. 1998. In vitro and in vivo evidence suggesting a role for iron in cisplatin-induced nephrotoxicity. *Kidney Int.* **53**:394–401.
9. Saad, S.Y., Najjar, T.A., and Al-Rikabi, A.C. 2001. The preventive role of deferoxamine against acute doxorubicin-induced cardiac, renal and hepatic toxicity in rats. *Pharmacol. Res.* **43**:211–218.
10. Paller, M.S., and Jacob, H.S. 1994. Cytochrome P-450 mediates tissue-damaging hydroxyl radical formation during reoxygenation of the kidney. *Proc. Natl. Acad. Sci. U. S. A.* **91**:7002–7006.
11. Baliga, R., Ueda, N., and Shah, S.V. 1993. Increase in bleomycin-detectable iron in ischaemia/reperfusion injury to rat kidneys. *Biochem. J.* **291**:901–905.
12. Baron, P., et al. 1991. Renal preservation after warm ischemia using oxygen free radical scavengers to prevent reperfusion injury. *J. Surg. Res.* **51**:60–65.
13. Alfrey, A.C. 1992. Toxicity of tubule fluid iron in the nephrotic syndrome. *Am. J. Physiol.* **263**:F637–F641.
14. Wu, Z.L., and Paller, M.S. 1994. Iron loading enhances susceptibility to renal ischemia in rats. *Ren. Fail.* **16**:471–480.
15. Walker, P.D., and Shah, S.V. 1988. Evidence suggesting a role for hydroxyl radical in gentamicin-induced acute renal failure in rats. *J. Clin. Invest.* **81**:334–341.
16. Paller, M.S., and Hedlund, B.E. 1988. Role of iron in postischemic renal injury in the rat. *Kidney Int.* **34**:474–480.
17. Paller, M.S., and Hedlund, B.E. 1994. Extracellular iron chelators protect kidney cells from hypoxia/reoxygenation. *Free Radic. Biol. Med.* **17**:597–603.
18. de Vries, B., et al. 2004. Reduction of circulating redox-active iron by apotransferrin protects against renal ischemia-reperfusion injury. *Transplantation.* **77**:669–675.
19. Zager, R.A., Burkhart, K.M., Conrad, D.S., and Gmur, D.J. 1995. Iron, heme oxygenase, and glutathione: effects on myohemoglobinuric proximal tubular injury. *Kidney Int.* **48**:1624–1634.
20. Horwitz, L.D., et al. 1998. Lipophilic siderophores of Mycobacterium tuberculosis prevent cardiac reperfusion injury. *Proc. Natl. Acad. Sci. U. S. A.* **95**:5263–5268.
21. Tacchini, L., Fusar Poli, D., Bernelli-Zazzera, A., and Cairo, G. 2002. Transferrin receptor gene expression and transferrin-bound iron uptake are increased during postischemic rat liver reperfusion. *Hepatology.* **36**:103–111.
22. Gunshin, H., et al. 1997. Cloning and characterization of a mammalian proton-coupled metal-ion transporter. *Nature.* **388**:482–488.
23. Hentze, M.W., et al. 1987. Identification of the iron-responsive element for the translational regulation of human ferritin mRNA. *Science.* **238**:1570–1573.
24. Leibold, E.A., and Munro, H.N. 1988. Cytoplasmic protein binds in vitro to a highly conserved sequence in the 5′ untranslated region of ferritin heavy- and light-subunit mRNAs. *Proc. Natl. Acad. Sci. U. S. A.* **85**:2171–2175.
25. Rouault, T.A., Hentze, M.W., Caughman, S.W., Harford, J.B., and Klausner, R.D. 1988. Binding of a cytosolic protein to the iron-responsive element of human ferritin messenger RNA. *Science.* **241**:1207–1210.
26. Eisenstein, R., and Blemings, K.P. 1998. Iron regulatory proteins, iron responsive elements and iron homeostasis. *J. Nutr.* **128**:2295–2298.
27. Rogers, J., and Munro, H. 1987. Translation of ferritin light and heavy subunit mRNAs is regulated by intracellular chelatable iron levels in rat hepatoma cells. *Proc. Natl. Acad. Sci. U. S. A.* **84**:2277–2281.
28. Ponka, P., Beaumont, C., and Richardson, D.R. 1998. Function and regulation of transferrin and ferritin. *Semin. Hematol.* **35**:35–54.
29. Wu, K.J., Polack, A., and Dalla-Favera, R. 1999. Coordinated regulation of iron-controlling genes, H-ferritin and IRP2, by c-MYC. *Science.* **283**:676–679.
30. Konijn, A.M., et al. 1999. The cellular labile iron pool and intracellular ferritin in K562 cells. *Blood.* **94**:2128–2134.
31. Ferris, C.D., et al. 1999. Haem oxygenase-1 prevents cell death by regulating cellular iron. *Nat. Cell Biol.* **1**:152–157.
32. Hanson, E.S., Rawlins, M.L., and Leibold, E.A. 2003. Oxygen and iron regulation of iron regulatory protein 2. *J. Biol. Chem.* **278**:40337–40342.
33. Hentze, M.W., and Kuhn, L.C. 1996. Molecular control of vertebrate iron metabolism: mRNA-based regulatory circuits operated by iron, nitric oxide, and oxidative stress. *Proc. Natl. Acad. Sci. U. S. A.* **93**:8175–8182.
34. Pantopoulos, K., and Hentze, M.W. 1998. Activation of iron regulatory protein-1 by oxidative stress in vitro. *Proc. Natl. Acad. Sci. U. S. A.* **95**:10559–10563.
35. Schalinske, K.L., and Eisenstein, R.S. 1996. Phosphorylation and activation of both iron regulatory proteins 1 and 2 in HL-60 cells. *J. Biol. Chem.* **271**:7168–7176.
36. Loncar, R., Flesche, C.W., and Deussen, A. 2004. Myocardial ferritin content is closely related to the degree of ischaemia. *Acta Physiol. Scand.* **180**:21–28.
37. Tacchini, L., Recalcati, S., Bernelli-Zazzera, A., and Cairo, G. 1997. Induction of ferritin synthesis in ischemic-reperfused rat liver: analysis of the molecular mechanisms. *Gastroenterology.* **113**:946–953.
38. Berberat, P.O., et al. 2003. Heavy chain ferritin acts as an antiapoptotic gene that protects livers from ischemia reperfusion injury. *FASEB J.* **17**:1724–1726.
39. Yang, J., et al. 2002. An iron delivery pathway mediated by a lipocalin. *Mol. Cell.* **10**:1045–1056.
40. Flower, D., North, A., and Sansom, C. 2000. The lipocalin family: structural and sequence overview. *Biochim. Biophys. Acta.* **1482**:9–24.
41. Goetz, D.H., et al. 2002. The neutrophil lipocalin NGAL is a bacteriostatic agent that interferes with siderophore-mediated iron acquisition. *Mol. Cell.* **10**:1033–1043.
42. Loomis, L.D., and Raymond, K.N. 1991. Solution equilibria of enterobactin and metal-enterobactin complexes. *Inorg. Chem.* **30**:906–911.
43. Li, J.Y., et al. 2004. Detection of intracellular iron by its regulatory effect. *Am. J. Physiol. Cell Physiol.* **287**:C1547–C1559.
44. Mishra, J., et al. 2003. Identification of neutrophil gelatinase–associated lipocalin as a novel early urinary biomarker for ischemic renal injury. *J. Am. Soc. Nephrol.* **14**:2534–2543.
45. Devarajan, P., Mishra, J., Supavekin, S., Patterson, L.T., and Potter, S. 2003. Gene expression in early ischemic renal injury: clues towards pathogenesis, biomarker discovery, and novel therapeutics. *Mol. Genet. Metab.* **80**:365–376.
46. Prozialeck, W.C., Lamar, P.C., and Appelt, D.M. 2004. Differential expression of E-cadherin, N-cadherin and beta-catenin in proximal and distal segments of the rat nephron. *BMC Physiol.* **4**:10–24.
47. Jablonski, P., et al. 1983. An experimental model for assessment of renal recovery from warm ischemia. *Transplantation.* **35**:198–204.
48. Bush, K.T., Tsukamoto, T., and Nigam, S.K. 2000. Selective degradation of E-cadherin and dissolution of E-cadherin-catenin complexes in epithelial ischemia. *Am. J. Physiol. Renal Physiol.* **278**:F847–F852.
49. Marambaud, P., et al. 2003. A CBP binding transcriptional repressor produced by the PS1/epsilon-cleavage of N-cadherin is inhibited by PS1 FAD mutations. *Cell.* **114**:635–645.
50. Leussink, B.T., et al. 2001. Loss of homotypic epithelial cell adhesion by selective N-cadherin displacement in bismuth nephrotoxicity. *Toxicol. Appl. Pharmacol.* **175**:54–59.

51. Jiang, J., Dean, D., Burghardt, R.C., and Parrish, A.R. 2004. Disruption of cadherin/catenin expression, localization, and interactions during HgCl2-induced nephrotoxicity. *Toxicol. Sci.* **80**:170–182.

52. Christensen, E.I., and Maunsbach, A.B. 1981. Dextran is resistant to lysosomal digestion in kidney tubules. *Virchows Arch., B, Cell Pathol.* **37**:49–59.

53. Axelsson, L., Bergenfeldt, M., and Ohlsson, K. 1995. Studies of the release and turnover of a human neutrophil lipocalin. *Scand. J. Clin. Lab. Invest.* **55**:577–588.

54. Sephton, R.G., Hodgson, G.S., De Abrew, S., and Harris, A.W. 1978. Ga67 and Fe59 distributions in mice. *J. Nucl. Med.* **19**:930–935.

55. Carrano, C.J., and Raymond, K.N. 1979. Ferric ion sequestering agents. II. Kinetics and mechanism of iron removal from transferrin by enterobactin and synthetic tricatechols. *J. Am. Chem. Soc.* **101**:5401–5404.

56. Nath, K.A., et al. 1992. Induction of heme oxygenase is a rapid, protective response in rhabdomyolysis in the rat. *J. Clin. Invest.* **90**:267–270.

57. Shimizu, H., et al. 2000. Protective effect of heme oxygenase induction in ischemic acute renal failure. *Crit. Care Med.* **28**:809–817.

58. Maines, M.D., Mayer, R.D., Ewing, J.F., and McCoubrey, W.K. 1993. Induction of kidney heme oxygenase-1 (HSP32) mRNA and protein by ischemia/reperfusion: possible role of heme as both promotor of tissue damage and regulator of HSP32. *J. Pharmacol. Exp. Ther.* **264**:457–462.

59. Fernandez-Pol, J.A. 1978. Isolation and characterization of a siderophore-like growth factor from mutants of SV40-transformed cells adapted to picolinic acid. *Cell.* **14**:489–499.

60. Jones, R., Peterson, C., Grady, R., and Cerami, A. 1980. Low molecular weight iron-binding factor from mammalian tissue that potentiates bacterial growth. *J. Exp. Med.* **151**:418–428.

61. Sturrock, A., Alexander, J., Lamb, J., Craven, C., and Kaplan, J. 1990. Characterization of a transferrin-independent uptake system for iron in HeLa cells. *J. Biol. Chem.* **265**:3139–3145.

62. Rosenthal, E.A., et al. 2001. An iron-binding exochelin prevents restenosis due to coronary artery balloon injury in a porcine model. *Circulation.* **104**:2222–2227.

63. Christensen, E.I., et al. 1999. Evidence for an essential role of megalin in transepithelial transport of retinol. *J. Am. Soc. Nephrol.* **10**:685–695.

64. Hilpert, J., et al. 2002. Related expression profiling confirms the role of endocytic receptor megalin in renal vitamin D3 metabolism. *Kidney Int.* **62**:1672–1681.

65. Borghoff, S.J., Short, B.G., and Swenberg, J.A. 1990. Biochemical mechanisms and pathobiology of alpha 2u-globulin nephropathy. *Annu. Rev. Pharmacol. Toxicol.* **30**:349–367.

66. Kozyraki, R., et al. 2001. Megalin-dependent cubilin-mediated endocytosis is a major pathway for the apical uptake of transferrin in polarized epithelia. *Proc. Natl. Acad. Sci. U. S. A.* **98**:12491–12496.

67. Cavaggioni, A., Findlay, J.B., and Tirindelli, R. 1990. Ligand binding characteristics of homologous rat and mouse urinary proteins and pyrazine-binding protein of calf. *Comp. Biochem. Physiol. B.* **96**:513–520.

68. Quadro, L., Hamberger, L., Colantuoni, V., Gottesman, M.E., and Blaner, W.S. 2003. Understanding the physiological role of retinol-binding protein in vitamin A metabolism using transgenic and knockout mouse models. *Mol. Aspects Med.* **24**:421–430.

69. Weichsel, A., Andersen, J.F., Champagne, D.E., Walker, F.A., and Montfort, W.R. 1998. Crystal structures of a nitric oxide transport protein from a blood-sucking insect. *Nat. Struct. Biol.* **5**:304–309.

70. Allhorn, M., Berggard, T., Nordberg, J., Olsson, M.L., and Akerstrom, B. 2002. Processing of the lipocalin alpha(1)-microglobulin by hemoglobin induces heme-binding and heme-degradation properties. *Blood.* **99**:1894–1901.

71. Fluckinger, M., Haas, H., Merschak, P., Glasgow, B.J., and Redl, B. 2004. Human tear lipocalin exhibits antimicrobial activity by scavenging microbial siderophores. *Antimicrob. Agents Chemother.* **48**:3367–3372.

72. Konopka, K., and Neilands, J.B. 1984. Effect of serum albumin on siderophore-mediated utilization of transferrin iron. *Biochemistry.* **23**:2122–2127.

73. O'Brien, I.G., Cox, G.B., and Gibson, F. 1970. Biologically active compounds containing 2,3-dihydroxybenzoic acid and serine formed by Escherichia coli. *Biochim. Biophys. Acta.* **201**:453–460.

74. Chipperfield, J.R., and Ratledge, C. 2000. Salicylic acid is not a bacterial siderophore: a theoretical study. *Biometals.* **13**:165–168.

75. Moerlein, S.M., Welch, M.J., Raymond, K.N., and Weitl, F.L. 1981. Tricatecholamide analogs of enterobactin as gallium- and indium-binding radiopharmaceuticals. *J. Nucl. Med.* **22**:710–719.

76. Emery, T., and Hoffer, P.B. 1980. Siderophore-mediated mechanism of gallium uptake demonstrated in the microorganism Ustilago sphaerogena. *J. Nucl. Med.* **21**:935–939.

77. Banin, E., Berenshtein, E., Kitrossky, N., Pe'er, J., and Chevion, M. 2000. Gallium-desferrioxamine protects the cat retina against injury after ischemia and reperfusion. *Free Radic. Biol. Med.* **28**:315–323.

78. Liang, M., Croatt, A.J., and Nath, K.A. 2000. Mechanisms underlying induction of heme oxygenase-1 by nitric oxide in renal tubular epithelial cells. *Am. J. Physiol. Renal Physiol.* **279**:F728–F735.

79. Gonzalez-Michaca, L., Farrugia, G., Croatt, A.J., Alam, J., and Nath, K.A. 2004. Heme: a determinant of life and death in renal tubular epithelial cells. *Am. J. Physiol. Renal Physiol.* **286**:F370–F377.

80. Poss, K.D., and Tonegawa, S. 1997. Reduced stress defense in heme oxygenase 1-deficient cells. *Proc. Natl. Acad. Sci. U. S. A.* **94**:10925–10930.

81. Nath, K.A., et al. 2000. The indispensability of heme oxygenase-1 in protecting against acute heme protein-induced toxicity in vivo. *Am. J. Pathol.* **156**:1527–1535.

82. Nath, K.A., et al. 2001. Heme protein-induced chronic renal inflammation: suppressive effect of induced heme oxygenase-1. *Kidney Int.* **59**:106–117.

83. Kanwar, Y.S. 2001. Heme oxygenase-1 in renal injury: conclusions of studies in humans and animal models. *Kidney Int.* **59**:378–379.

84. Agarwal, A., Balla, J., Alam, J., Croatt, A.J., and Nath, K.A. 1995. Induction of heme oxygenase in toxic renal injury: a protective role in cisplatin nephrotoxicity in the rat. *Kidney Int.* **48**:1298–1307.

85. Ohta, K., et al. 2000. Tubular injury as a cardinal pathologic feature in human heme oxygenase-1 deficiency. *Am. J. Kidney Dis.* **35**:863–870.

86. Poss, K.D., and Tonegawa, S. 1997. Heme oxygenase 1 is required for mammalian iron reutilization. *Proc. Natl. Acad. Sci. U. S. A.* **94**:10919–10924.

87. Sikorski, E.M., Hock, T., Hill-Kapturczak, N., and Agarwal A. 2004. The story so far: molecular regulation of the heme oxygenase-1 gene in renal injury. *Am. J. Physiol. Renal Physiol.* **286**:F425–F441.

88. Inguaggiato, P., et al. 2001. Cellular overexpression of heme oxygenase-1 up-regulates p21 and confers resistance to apoptosis. *Kidney Int.* **60**:2181–2191.

89. Hodges, Y.K., Antholine, W.E., and Horwitz, L.D. 2004. Effect on ribonucleotide reductase of novel lipophilic iron chelators: the desferri-exochelins. *Biochem. Biophys. Res. Commun.* **315**:595–598.

90. Alcantara, O., Kalidas, M., Baltathakis, I., and Boldt, D.H. 2001. Expression of multiple genes regulating cell cycle and apoptosis in differentiating hematopoietic cells is dependent on iron. *Exp. Hematol.* **29**:1060–1069.

91. Ye, Z., and Connor, J.R. 2000. Identification of iron responsive genes by screening cDNA libraries from suppression subtractive hybridization with antisense probes from three iron conditions. *Nucleic Acids Res.* **28**:1802–1807.

92. Kim, B.S., et al. 2002. Involvement of p38 MAP kinase during iron chelator-mediated apoptotic cell death. *Cell. Immunol.* **220**:96–106.

93. Chong, T.W., Horwitz, L.D., Moore, J.W., Sowter, H.M., and Harris, A.L. 2002. A mycobacterial iron chelator, desferri-exochelin, induces hypoxia-inducible factors 1 and 2, NIP3, and vascular endothelial growth factor in cancer cell lines. *Cancer Res.* **62**:6924–6927.

94. Devireddy, L.R., Teodoro, J.G., Richard, F.A., and Green, M.R. 2001. Induction of apoptosis by a secreted lipocalin that is transcriptionally regulated by IL-3 deprivation. *Science.* **293**:829–834.

95. Markowitz, G.S., et al. 2003. Toxic acute tubular necrosis following treatment with zoledronate (Zometa). *Kidney Int.* **64**:281–289.

96. Bundgaard, J.R., Sengelov, H., Borregaard, N., and Kjeldsen, L. 1994. Molecular cloning and expression of a cDNA encoding NGAL: a lipocalin expressed in human neutrophils. *Biochem. Biophys. Res. Commun.* **202**:1468–1475.

97. Lee, H.T., Xu, H., Nasr, S.H., Schnermann, J., and Emala, C.W. 2004. A1 adenosine receptor knockout mice exhibit increased renal injury following ischemia and reperfusion. *Am. J. Physiol. Renal Physiol.* **286**:F298–F306.

98. Vogel, S., et al. 2002. Retinol-binding protein-deficient mice: biochemical basis for impaired vision. *Biochemistry.* **41**:15360–15368.

99. Maines, M.D. 1981. Zinc protoporphyrin is a selective inhibitor of heme oxygenase activity in the neonatal rat. *Biochim. Biophys. Acta.* **673**:339–350.

100. Heinegard, D., and Tiderstrom, G. 1973. Determination of serum creatinine by a direct colorimetric method. *Clin. Chim. Acta.* **43**:305–310.